Light-front QCD. III. Coupling constant renormalization

Avaroth Harindranath* and Wei-Min Zhang†
Department of Physics, The Ohio State University, Columbus, Ohio 43210
(Received 10 June 1993)

In this third part in a series of papers on light-front QCD, we continue the study of regularization and renormalization in old-fashioned perturbative light-front formalism. We calculate lowest order radiative corrections to the quark-gluon coupling constant in light-front QCD. An attempt is made to understand the origin of antiscreening in a formulation of QCD with *only* physical degrees of freedom in terms of contributions from distinct Fock space sectors. The relevance of our results to bound state calculations in QCD with a truncated Fock space are discussed.

PACS number(s): 11.10.Ef, 11.10.Gh, 12.38.Bx

I. INTRODUCTION

The old fashioned idea [1] of applying Tamm-Dancoff methods to light-front Hamiltonians in field theory has received some revival recently [2,3]. Most of the recent work has been devoted to the study of two-dimensional models. The ultimate objective of this enterprise is to study bound states in QCD. However, methods to solve light-front QCD Hamiltonian (QCD Hamiltonian in light-front coordinates in light-front gauge $A^+ = 0$) are still in their infancy. One major obstacle to progress comes from infrared and ultraviolet problems that plague light-front QCD.

In a series of papers [4–6] we have begun a systematic study of light-front QCD. We are particularly interested in Fock space methods involving few degrees of freedom. A straightforward diagonalization of the canonical light-front Hamiltonian in a few-body Fock space will lead to severe infrared and ultraviolet divergences. These divergences are strongly regulator dependent and an understanding of this regulator dependence is essential before one can extract sensible numbers out of any numerical calculations. Note that the renormalization problem is much more intricate in QCD compared to QED, especially since the elementary degrees of freedom that appear in the Hamiltonian do not appear as physical states.

In Ref. [6] (hereafter referred to as paper II) we started an extensive study of regularization and renormalization in old-fashioned light-front QCD perturbation theory. Since we are interested in both perturbative and nonperturbative aspects, we have studied the implications of a variety of cutoffs. We have evaluated the corrections to quark mass and wave function renormalizations using different regularization schemes. We have also studied the counterterms required for gluon mass and wave function renormalizations. In the present work we study the problem of renormalization of the coupling constant. A brief summary of the results has been presented in Ref. [7].

Our study of coupling constant renormalization is partly motivated by the investigation of the manifestation of asymptotic freedom in different gauges. The study of asymptotic freedom in non-Abelian gauge theory has a long history [8]. The celebrated first calculations [9,10] were done in covariant gauges. In covariant gauges, loop contributions from Faddeev-Popov ghosts are a necessary ingredient to ensure the correct coefficient which determines the approach to asymptotic freedom. In Coulomb gauge, ghosts are not involved in the lowest order and asymptotic freedom arises from a diagram involving both transverse and Coulomb gluons [11–14]. In axial gauge $A^3 = 0$ (which has some similarities to light-front gauge $A^+ = 0$), Faddeev-Popov ghosts are decoupled to all orders but the gauge propagator contains severe $\frac{1}{q\cdot\eta}$ and $\frac{1}{(q\cdot\eta)^2}$ singularities where q is the gauge boson momentum and η is the spacelike vector characterizing the axial gauge. With the prescription for the double pole which is *defined* to be obtained by the differentiation of the principal value prescription for the single pole, the correct value is obtained for the ultraviolet divergent part of the gluon wave function renormalization constant [12,15]. As noted by Frenkel and Taylor [12] the crucial fact is that the gluon spectral function, which is formally positive, receives a negative contribution because of the $\frac{1}{(q_3)^2}$ gauge singularity in $A^3 = 0$ gauge, and this in turn causes antiscreening.

Previous calculations in light-front gauge can be classified into four different categories. The earliest calculation by Thorn [16] was done for the pure Yang-Mills theory in the context of four-dimensional loop integrals with noncovariant regularization (k^- integration first, and separate cutoffs for k^+ and $k^\perp$). Thorn studied the four-gluon vertex for the kinematic choice of zero external transverse momenta and arrived at the well-known result for the running coupling constant. As a part of developing calculational techniques to study the evolution of hadronic structure functions, Curci, Furmanski, and Petronzio [17] studied radiative corrections to the quark-gluon vertex in $A^+ = 0$ gauge. These authors con-

*Electronic address: hari@mps.ohio-state.edu
†Electronic address: wzhang@mps.ohio-state.edu

sidered massless quarks and employed dimensional regularization as the ultraviolet regulator and a principal value prescription for $\frac{1}{k^+}$ gauge singularity. They also utilized an "infinite-momentum parametrization" of the momenta [18]. As a consequence of the principal value prescription, various renormalization "constants" depend on longitudinal momenta. In addition, various renormalization constants contain products of ultraviolet regulator and the principal value regulator (the so-called mixing problem). This mixing is an inevitable consequence of Hamiltonian field theory with only physical degrees of freedom as emphasized by Thorn who first observed this effect. In the calculation of Curci *et al.*, however, when all the renormalization constants are collected to compute the radiative correction to the coupling constant, the unwanted products all cancel and one recovers the well-known running coupling constant. There exist also calculations which utilize four-dimensional integrals and choose the Mandelstam-Leibbrandt prescription [19,20] for the gauge singularity and dimensional regularization for the ultraviolet divergence. In this context there have been formulations where (a) the unphysical gauge degrees of freedom are explicitly eliminated in the Lagrangian using the constraint equations (for the case of pure Yang-Mills theory see [21,22]) and (b) the unphysical gauge degrees of freedom are kept [23]. In the former case, because of gauge fixing, one can no longer verify Slavnov-Taylor identities but the loop calculations are very simple and renormalizability is quite transparent. In the latter case, since the residual gauge freedom is kept, one can explicitly verify Slavnov-Taylor identities even though loop calculations are very complicated and the discussion of renormalizability is quite intricate. For an excellent discussion of the two formalisms for Yang-Mills theory see Ref. [22]. The Mandelstam-Leibbrandt (ML) prescription, which is essential for the success of these approaches, makes Wick rotation and Euclidean power counting possible for four-dimensional loop integrals in Feynman perturbation theory. The ML prescription as such cannot be applied to Hamiltonian perturbation theory [24]. In old-fashioned light-front perturbation theory, one has to deal with three-dimensional noncovariant integrals, and furthermore the light-front power counting is very different from equal-time power counting [25]. Hence there is no *a priori* reason to abandon the principal value prescription in old-fashioned light-front perturbation theory. One should study in detail the criteria for renormalizability in the Hamiltonian framework. As a starting point one should investigate the cancellation of gauge singularities in physically relevant quantities. The study of the renormalization of the quark-gluon coupling in QCD in lowest order offers this opportunity.

A further motivation to investigate the running of the coupling constant in light-front gauge in old-fashioned perturbation theory arises from the study of high-energy inclusive and exclusive reactions in QCD. As is well known (see, for example, Refs. [27,17,28]), in order to have a successful partonic interpretation of these physical processes it is essential to work in gauges where the gluon has only physical degrees of freedom. Furthermore, as Drell, Levy, and Yan [29] and Bjorken, Kogut, and Soper [30] have argued, old-fashioned perturbation theory and the triviality of vacuum are essential ingredients for a probabilistic interpretation of parton densities. In order to develop a perturbative approach to exclusive reactions in QCD, as Brodsky and Lepage [31] have emphasized, the formalism of old-fashioned perturbation theory and light-front quantization are very convenient tools. Thus a study of the origin of antiscreening in light-front QCD utilizing old-fashioned perturbation theory in the Hamiltonian context (which employs only physical degrees of freedom) becomes extremely relevant for the systematic calculation of physical processes in high-energy QCD.

A further motivation to study renormalization of the coupling constant in light-front QCD comes from our ultimate objective of studying bound states in QCD. The relativistic bound-state equations require regularization and renormalization. The renormalization procedure requires us to take the cutoff to be much larger than the mass scales of the bound states. In theories that lack asymptotic freedom, larger cutoffs imply small renormalized couplings and weak effective couplings in the low-momentum region. This results in almost nonrelativistic bound states or even no bound states (triviality problem). An example of this phenomenon is provided in Ref. [32]. A theory that possesses asymptotic freedom may help us to perform renormalization in a more meaningful manner by allowing us to choose cutoffs to be much larger than bound-state mass scales. Furthermore, in such a theory the effective coupling grows at small momenta irrespective of the value of the renormalized coupling, and the possibility arises for building strongly bound states irrespective of even weak renormalized coupling. However, just the knowledge that the theory possesses asymptotic freedom is no guarantee that renormalization may be carried out in a simple manner in a bound-state calculation. This is because in practice, we have to truncate the Fock space in order to make the numerical problem tractable on a computer. Since Feynman diagrams hide multiparticle intermediate states behind covariant propagators, what minimal Fock space states are to be included in order to overcome the triviality problem is obscure in the context of covariant calculations. This issue is naturally resolved in the old-fashioned Hamiltonian perturbation theory calculations.

The plan of this paper is as follows. In Sec. II we discuss the structure of the quark-gluon vertex for different kinematical choices and specify some characteristic features of the calculation. Radiative corrections to the vertex for zero external gluon momentum are discussed in Sec. III. The corrections to helicity-flip matrix elements are discussed in Sec. IV. Section V contains the discussion, conclusions, and outlook. The explicit expressions for various diagrams contributing to coupling constant renormalization using the rules we developed in paper II are presented in the Appendix.

II. QUARK-GLUON VERTEX IN LIGHT-FRONT QCD

The canonical light-front Hamiltonian contains several different three-point and four-point interactions and *a*

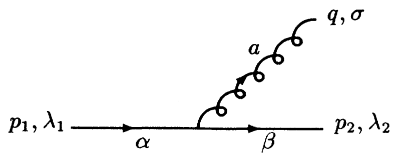

FIG. 1. The lowest order quark-gluon vertex in QCD.

priori there is no reason to assume that the strengths of the various interactions will renormalize in the same manner. In principle one should study the evolution of the strengths of all the interactions that appear in the Hamiltonian. In the present paper we do not undertake this ambitious program. Instead we study one particular quark-gluon vertex, the one arising from the three-point interaction. We investigate radiative corrections to this vertex for different choices of external momenta.

The lowest order three-point quark-gluon interaction matrix element (Fig. 1) is given by

$$\mathcal{M}_0 = -g\, T^a_{\beta\alpha}\, \chi^\dagger_{\lambda_2} \left[\frac{2q^i}{q^+} - \frac{\sigma^\perp \cdot p_2^\perp}{p_2^+}\sigma^i - \sigma^i \frac{\sigma^\perp \cdot p_1^\perp}{p_1^+} + im\left(\frac{1}{p_2^+} - \frac{1}{p_1^+}\right)\sigma^i \right] \chi_{\lambda_1}\, \epsilon^{i*}_\sigma . \tag{2.1}$$

In the above equation and in the rest of the paper the factor $\frac{1}{k^+}$, where k^+ is any longitudinal momentum has the principal value prescription, i.e., $\frac{1}{k} \to \frac{1}{2}(\frac{1}{k+i\epsilon} + \frac{1}{k-i\epsilon})$, denoted $\frac{1}{[k]}$ in paper II. If we set $q(q^+, q^\perp) = 0$, the matrix element is (since $p_1^{i,+} = p_2^{i,+} = p^{i,+}$)

$$\mathcal{M}_{01} = 2\, g\, T^a_{\beta\alpha}\, \frac{p^i}{p^+} \delta_{\lambda_1\lambda_2} \epsilon^{i*}_\sigma . \tag{2.2}$$

From the structure of this vertex we expect the one-loop corrections to be of the form

$$\delta\mathcal{M}_{01} = 2\, \delta g\, T^a_{\beta\alpha}\, \frac{p^i}{p^+} \delta_{\lambda_1\lambda_2} \epsilon^{i*}_\sigma . \tag{2.3}$$

If we set all external transverse momenta to zero, only the helicity-flip part of the matrix element survives:

$$\mathcal{M}_{02} = img\, T^a_{\beta\alpha} \left(\frac{1}{p_1^+} - \frac{1}{p_2^+}\right) \chi^\dagger_{\lambda_2} \sigma^i \chi_{\lambda_1} \epsilon^{i*}_\sigma . \tag{2.4}$$

Since mass m and g appear in this vertex multiplicatively, we expect the vertex correction to be of the form

$$\delta\mathcal{M}_{02} = i\Big(m\delta g + g\delta m\Big)\, T^a_{\beta\alpha} \left(\frac{1}{p_1^+} - \frac{1}{p_2^+}\right) \chi^\dagger_{\lambda_2} \sigma^i \chi_{\lambda_1} \epsilon^{i*}_\sigma . \tag{2.5}$$

Thus we expect in addition to the coupling constant renormalization a "vertex mass" correction also occurring due to radiative corrections. In the following we study the radiative corrections to both the matrix elements $\mathcal{M}_{01}$ and $\mathcal{M}_{02}$. We will see that the contributions of various time-ordered diagrams depend crucially on the kinematical choice of external momenta. The calculations simplify drastically for the choice of zero external gluon momentum. However, it is important to note that this kinematic choice cannot be made *a priori* for the contribution arising from the gluon wave function renormalization constant. Naively, this contribution seems to vanish automatically for zero longitudinal momentum (q^+) of the external gluon since it is the upper limit of loop longitudinal momentum. However, the integrand has a $\frac{1}{q^+}$ factor with the consequence that the result after the integration for nonzero q^+ is finite in the limit $q^+ \to 0$. The study of radiative corrections to $\mathcal{M}_{02}$ is especially interesting following the observation [25] that *in light-front quantization in 3+1 dimensions, chirality is the same as helicity.* $\mathcal{M}_{02}$ is the only helicity-flip interaction in the entire canonical light-front QCD Hamiltonian. The coupling constant and the quark mass enter multiplicatively in this vertex. Thus a separate identification of the "vertex mass counterterm" is necessary in order to isolate the radiative corrections to the coupling constant. The difference between the vertex mass and the kinetic mass (the mass that appears in the free part of the Hamiltonian) has been emphasized and discussed in detail previously by Burkardt and Langnau [26] in the context of renormalization of Yukawa model and QED. Note that the mass counterterm (which preserves particle number) is quadratic in the quark mass whereas the "vertex mass counterterm" (which changes particle number) is linear in the quark mass.

The one-loop vertex correction diagrams are given in Figs. 2–7. The corresponding expressions using the rules of old-fashioned perturbation theory are collected in the Appendix. Details of the rules developed in a two-component formalism are given in paper II. The computations using these are simpler compared to those using a four-component formalism [31]. For the loop integrals we have chosen the simplest regularization scheme, namely, we use the principal value prescription for k^+ and a low and high cutoff for $k^\perp$ ($\mu < k^\perp < \Lambda$) with μ much greater than all particle masses. To avoid singularities we have kept the initial quark state off its mass shell and P_1^- denotes the off-mass shell light-front energy. Note that Figs. 2 and 3 receive contributions from both the mass correction and the wave function renormalization constant correction. In these cases we first extract the divergences by expanding the energy denominators. To be specific, for example, for Fig. 1(a) we find the product of energy denominators:

$$\frac{1}{\mathrm{ED}} \equiv \frac{1}{P^- - p_1^-}\frac{1}{P^- - k^- - (p_1 - k)^-} = \frac{1}{P^- - p_1^-}A(P^-)$$
$$= \frac{1}{P^- - p_1^-}\left(A(P^- = p_1^-) + (P^- - p_1^-)\left.\frac{\partial A(P^-)}{\partial P^-}\right|_{P^- = p_1^-} + \cdots\right). \quad (2.6)$$

In this expansion, the first term corresponds to the mass correction and is subtracted by a mass counterterm. It is the second term which has ultraviolet logarithmic divergences that contributes to the renormalization of the coupling constant. In the rest of the paper (except the Appendix) for Figs. 2 and 3 we explicitly give only the expression for the second term in the above expansion.

Note that we have used the identities

$$(T^aT^a)_{\beta\alpha} = C_f\delta_{\beta\alpha}, \quad (2.7)$$
$$\mathrm{Tr}(T^aT^b) = T_f\delta_{ab} = \tfrac{1}{2}\delta_{ab}, \quad (2.8)$$
$$T^bT^aT^b = (-\tfrac{1}{2}C_A + C_f)T^a, \quad (2.9)$$
$$if_{abc}T^bT^c = -\tfrac{1}{2}C_AT^a, \quad (2.10)$$

where $C_f = \frac{N^2-1}{2N}$ and $C_A = N$ for SU(N).

III. RADIATIVE CORRECTIONS TO $\mathcal{M}_{01}$

If we set external gluon momentum $q(q^+, q_\perp^i) = 0$, the quark-gluon vertex is reduced to Eq. (2.2). In x^+-ordered perturbation theory, the one-loop vertex correction is given by

$$\delta\mathcal{M}_{01} = \{M_2 + M_3 + M_4 + M_5 + M_6 + M_7\}\mathcal{M}_{01}, \quad (3.1)$$

where $M_n, n = 2$–7 are represented by Figs. 2–7 and the corresponding expressions are given in the Appendix.

Figure 2 receives a contribution from fermion wave function renormalization. The contribution from Fig. 2(a) is

$$M_{2(\mathrm{a})} = \frac{g^2}{4\pi^2}\left(\frac{3}{2} - 2\ln\frac{p^+}{\epsilon}\right)C_f \ln\frac{\Lambda}{\mu}\,. \quad (3.2)$$

Here we first encounter the infamous mixing of ultraviolet and infrared divergences. In the Hamiltonian context there is nothing unnatural about this result since in old-fashioned perturbation theory with a trivial vacuum, we expect the second-order contribution to wave function renormalization to be negative, as explained in paper II. The contribution from Fig. 2(b) is

$$M_{2(\mathrm{b})} = \frac{g^2}{4\pi^2}\left(\frac{3}{2} - 2\ln\frac{p^+}{\epsilon}\right)C_f \ln\frac{\Lambda}{\mu}. \quad (3.3)$$

The sum of contributions from Figs. 2(a) and 2(b) is

$$M_2 = \{M_{2(\mathrm{a})} + M_{2(\mathrm{b})}\}$$
$$= \frac{g^2}{2\pi^2}\left(\frac{3}{2} - 2\ln\frac{p^+}{\epsilon}\right)C_f \ln\frac{\Lambda}{\mu}. \quad (3.4)$$

Next we calculate the contributions from the gluon wave function renormalization. We emphasize that for Fig. 3 one has to be very careful for the choice of $q^+ = 0$.

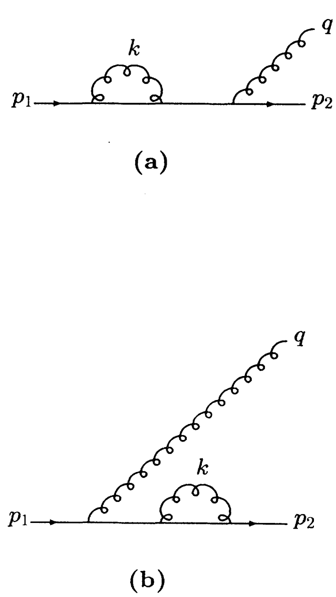

FIG. 2. Contribution to quark-gluon vertex from fermion wave function renormalization.

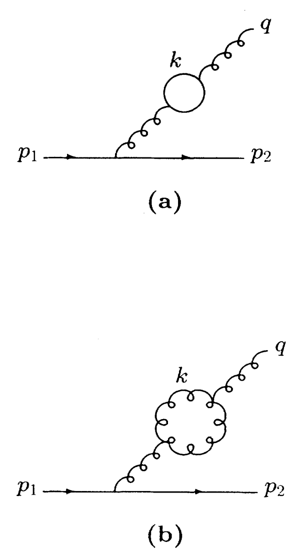

FIG. 3. Contribution to quark-gluon vertex from gluon wave function renormalization.

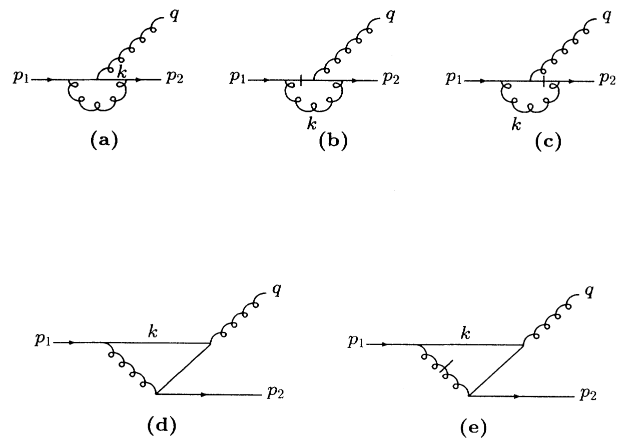

FIG. 4. Contribution to quark-gluon vertex from different time-ordering diagrams all of which correspond to a single Feynman diagram for vertex correction involving quark-gluon vertex.

With the principal value prescription, $\frac{k^+}{k^+} = 1$ at $k^+ \to 0$, which implies that the integral $\frac{1}{q^+}\int_0^{q^+} dk^+$ involved in Fig. 3 is not simply zero. Here we set $q^+ = 0$ after the integration. Obviously, Figs. 3(a) and 3(b) are the wave function renormalization corrections to the emitted gluon, similar to the quark wave function renormalization in Fig. 2. It is easy to find that

$$M_{3(a)} = -\frac{g^2}{8\pi^2}\frac{4}{3}N_f T_f \ln\frac{\Lambda}{\mu}\,, \tag{3.5}$$

$$M_{3(b)} = \frac{g^2}{8\pi^2}\frac{11}{3}C_A \ln\frac{\Lambda}{\mu}\,. \tag{3.6}$$

Thus,

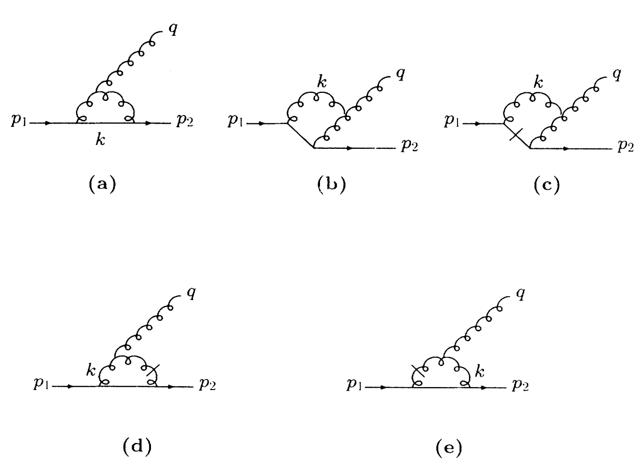

FIG. 5. Contribution to quark-gluon vertex from different time-ordering diagrams all of which correspond to a single Feynman diagram for vertex correction involving three-gluon vertex.

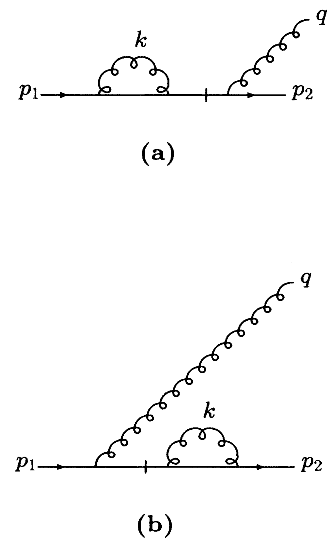

FIG. 6. Contribution to quark-gluon vertex involving instantaneous fermion interaction that does not change particle number.

$$\begin{aligned} M_3 &= M_{3(a)} + M_{3(b)} \\ &= \frac{g^2}{8\pi^2}\left(\frac{11}{3}C_A - \frac{4}{3}N_f T_f\right). \end{aligned} \tag{3.7}$$

The contribution from the intermediate fermion-antifermion pair is free of gauge singularities and is negative as expected. The contribution from the intermediate two-gluon state is expected to be affected by the infrared singularity and negative as anticipated from second order perturbation theory [see Eq. (4.6)]. However, the infrared logarithmic divergences in the gluon wave function renormalization constant are removed due to $q^+ = 0$.

Next consider contributions from Fig. 4:

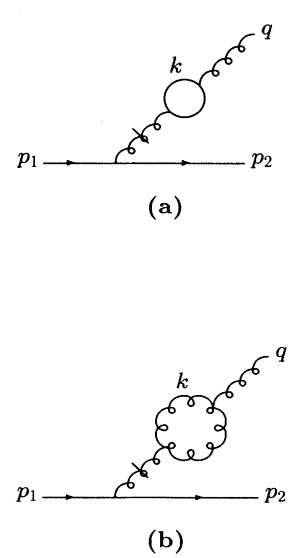

FIG. 7. Contribution to quark-gluon vertex involving an instantaneous gluon.

$$M_{4(\mathrm{a})} = 2\, g^2 \left(-\frac{1}{2}C_A + C_f\right) \int \frac{d^2\kappa}{2(2\pi)^3}\frac{1}{\kappa^2} \int_0^{p^+} \frac{dk^+}{p^+}\left(2\frac{p^+}{k^+} - 2 + \frac{k^+}{p^+}\right)$$
$$= -\frac{g^3}{4\pi^2}\left(\frac{3}{2} - 2\ln\frac{p^+}{\epsilon}\right)\left(-\frac{1}{2}C_A + C_f\right)\ln\frac{\Lambda}{\mu}\,, \tag{3.8}$$

$$M_{4(\mathrm{b})} = M_{4(\mathrm{c})} = M_{4(\mathrm{d})} = M_{4(\mathrm{e})} = 0\,. \tag{3.9}$$

Here $M_{4(\mathrm{d})}$ and $M_{4(\mathrm{e})}$ have zero contribution to the vertex correction because these two diagrams vanish for $q^+ = 0$ due to the positivity of light-front longitudinal momentum. Thus,

$$M_4 = -\frac{g^2}{4\pi^2}\left(\frac{3}{2} - 2\ln\frac{p^+}{\epsilon}\right)\left(-\frac{1}{2}C_A + C_f\right)\ln\frac{\Lambda}{\mu}\,. \tag{3.10}$$

Next we consider contributions from Fig. 5:

$$M_{5(\mathrm{a})} = -2\, g^2\left(\frac{-1}{2}\right)C_A \int \frac{d^2\kappa}{2(2\pi)^3}\frac{1}{\kappa^2}\int_0^{p^+}\frac{dk^+}{p^+}\left(2\frac{p^+}{k^+} - 2 + \frac{k^+}{p^+}\right)$$
$$= -\frac{g^2}{8\pi^2}C_A\left(\frac{3}{2} - 2\ln\frac{p^+}{\epsilon}\right)\ln\frac{\Lambda}{\mu}\,, \tag{3.11}$$

$$M_{5(\mathrm{b})} = 0\,, \tag{3.12}$$

$$M_{5(\mathrm{c})} = 0\,, \tag{3.13}$$

$$M_{5(\mathrm{d})}\mathcal{M}_{01} = 2g^3\frac{-1}{2}C_A T^a_{\beta\alpha}\frac{(\chi^\dagger_{\lambda_2}\sigma^i\chi_{\lambda_1})\epsilon^{i*}im}{p^+}\int\frac{d^2\kappa}{2(2\pi)^3\kappa^2}\int_0^{p^+}\frac{dk^+}{p^+}$$
$$= -\frac{g^3}{8\pi^2}\frac{(\chi^\dagger_{\lambda_2}i\sigma^i\chi_{\lambda_1})\epsilon^{i*}m}{p^+}T^a_{\beta\alpha}C_A\ln\frac{\Lambda}{\mu}$$
$$= -M_{5(\mathrm{e})}\mathcal{M}_{01}\,. \tag{3.14}$$

So

$$M_5 = \{M_{5(\mathrm{a})} + M_{5(\mathrm{b})} + M_{5(\mathrm{c})} + M_{5(\mathrm{d})} + M_{5(\mathrm{e})}\}$$
$$= -\frac{g^2}{8\pi^2}\left(\frac{3}{2} - 2\ln\frac{p^+}{\epsilon}\right)C_A\ln\frac{\Lambda}{\mu}. \tag{3.15}$$

The contribution from Fig. 6 is

$$M_{6(\mathrm{a})}\mathcal{M}_{01} = 2g^3 T^a_{\beta\alpha}C_f\frac{(\chi^\dagger_{\lambda_2}i\sigma^i\chi_{\lambda_1})\epsilon^{i*}m}{p^+}$$
$$\times\int\frac{d^2\kappa}{2(2\pi)^3}\frac{1}{\kappa^2}\int_0^{p^+}dk^+\frac{k^+}{p^{+2}}$$
$$= \frac{g^3}{4\pi^2}T^a_{\beta\alpha}\frac{(\chi^\dagger i\sigma^i\chi)\epsilon^{i*}m}{p^+}C_f\ln\frac{\Lambda}{\mu}$$
$$= -M_{6(\mathrm{b})}\mathcal{M}_{01}. \tag{3.16}$$

Thus the total contribution from Figs. 6(a) and 6(b) is

$$M_6 = 0. \tag{3.17}$$

For Fig. 7, we make the kinematical choice after the evaluation of the diagram. The contributions from Fig. 7 are

$$M_{7(\mathrm{a})} = M_{7(\mathrm{b})} = 0. \tag{3.18}$$

To evaluate the contributions to the coupling constant we have to multiply M_2 and M_3 by $\frac{1}{2}$ in order to take into account the proper correction due to the renormalization of initial and final states [33,34] [also see Eq. (3.33) in paper II]. Thus adding the contributions we have

$$\delta\mathcal{M}_{01} = (\tfrac{1}{2}M_2 + \tfrac{1}{2}M_3 + M_4 + M_5 + M_6 + M_7)\mathcal{M}_{01}$$
$$= \mathcal{M}_{01}\frac{g^2}{8\pi^2}\left(\frac{11}{6}C_A - \frac{2}{3}N_f T_f\right)\ln\frac{\Lambda}{\mu}. \tag{3.19}$$

Note that all mixed divergences cancel. The correction to the coupling constant is given by

$$g_R = g(1 + \delta g) = g\left[1 + \frac{g^2}{8\pi^2}\left(\frac{11}{6}C_A - \frac{2}{3}N_f T_f\right)\ln\frac{\Lambda}{\mu}\right]. \tag{3.20}$$

We compute the β function by

$$\beta(g) = -\frac{\partial g_R}{\partial\ln\Lambda} \tag{3.21}$$

$$= -\frac{g^3}{16\pi^2}\left(\frac{11}{3}C_A - \frac{4}{3}N_f T_f\right)\,, \tag{3.22}$$

which is the well-known result to the one-loop order.

IV. RADIATIVE CORRECTIONS TO $\mathcal{M}_{02}$

In this section we present the results for the lowest order radiative corrections to the strength of the helicity-flip matrix element in light-front QCD using the old-fashioned perturbation theory rules given in paper II. We present the results for each time-ordered diagram separately in order to exhibit the contribution from distinct intermediate Fock-space states.

The one-loop vertex correction is given by

$$\delta\mathcal{M}_{02} = \left\{M_2 + M_3 + M_4 + M_5 + M_6 + M_7\right\} \mathcal{M}_{02}. \tag{4.1}$$

First we give the contributions from fermion wave function renormalization. The time-ordered diagrams are given in Figs. 2(a) and 2(b). The corresponding expressions are given in the Appendix. The contribution from Fig. 2(a) is

$$M_{2(\mathrm{a})} = (-)\frac{g^2}{4\pi^2}\,C_F\left(2\ln\frac{p_1^+}{\epsilon} - \frac{3}{2}\right)\ln\frac{\Lambda}{\mu}. \tag{4.2}$$

The contribution from Fig. 2(b) is

$$M_{2(\mathrm{b})} = (-)\frac{g^2}{4\pi^2}\,C_f\left(2\ln\frac{p_2^+}{\epsilon} - \frac{3}{2}\right)\ln\frac{\Lambda}{\mu}. \tag{4.3}$$

The combined contribution from Fig. 2 is

$$M_2 = (-)\frac{g^2}{4\pi^2}\,C_f\left(2\ln\frac{p_1^+p_2^+}{\epsilon^2} - 3\right)\ln\frac{\Lambda}{\mu}. \tag{4.4}$$

Next we calculate the contributions from the gluon wave function renormalization constant. The time-ordered diagrams are given in Figs. 3(a) and 3(b). The contributions from fermion-antifermion intermediate states are given by

$$M_{3(\mathrm{a})} = (-)\;2\;N_f\;T_f\;\frac{g^2}{2(2\pi)^3}\int\frac{d^2\kappa}{\kappa^2}\times\frac{1}{q^+}\int_0^{q^+} dk^+\,\frac{(k^+)^2 + (q^+ - k^+)^2}{(q^+)^2} = N_f\;T_f\;(-)\frac{g^2}{6\pi^2}\ln\frac{\Lambda}{\mu}. \tag{4.5}$$

We have assumed that there are N_f flavors of fermions. Note that this contribution is the same as that for the kinematical choice $q^+ = 0$.

The contributions from two-gluon intermediate states are given by

$$M_{3(\mathrm{b})} = C_A(-)\frac{g^2}{(2\pi)^3}\int\frac{d^2\kappa}{\kappa^2}\frac{1}{q^+}\int_0^{q^+} dk^+ k^+(q^+ - k^+)\left[\frac{1}{(k^+)^2} + \frac{1}{(q^+ - k^+)^2} + \frac{1}{(q^+)^2}\right] = \frac{1}{2}\;C_A\;\frac{g^2}{4\pi^2}\left(\frac{11}{3} - 4\ln\frac{q^+}{\epsilon}\right)\ln\frac{\Lambda}{\mu}. \tag{4.6}$$

The two-gluon intermediate state contribution is negative, as one expects from old-fashioned perturbation theory, solely due to the presence of mixing term. We reiterate that this a natural feature of Hamiltonian calculations with only physical degrees of freedom.

Next we consider contributions from Fig. 4. The contribution from Fig. 4(a) is

$$M_{4(\mathrm{a})} = 4\left(-\frac{1}{2}C_A + C_f\right)\frac{g^2}{2(2\pi)^3}\int\frac{d^2\kappa}{\kappa^2}\int_0^{p_2^+} dk^+\left(\frac{1}{p_2^+ - k^+} + \frac{k^+}{2p_1^+p_2^+} + \frac{1}{2p_2^+}\right) = -\left(-\frac{1}{2}C_A + C_f\right)\frac{g^2}{2\pi^2}\left(\ln\frac{\epsilon}{p_2^+} - \frac{1}{2} - \frac{1}{4}\frac{p_2^+}{p_1^+}\right)\ln\frac{\Lambda}{\mu}. \tag{4.7}$$

The contribution from Fig. 4(b) is

$$M_{4(\mathrm{b})} = 0. \tag{4.8}$$

The contribution from Fig. 4(c) is

$$M_{4(\mathrm{c})} = 0. \tag{4.9}$$

The contribution from Fig. 4(d) is

$$M_{4(\mathrm{d})} = \left(-\frac{1}{2}C_A + C_f\right)4\frac{p_2^+}{q^+}\frac{g^2}{2(2\pi)^3}\int\frac{d^2\kappa}{\kappa^2}\int_0^{q^+} dk^+\frac{k^+}{p_1^+ - k^+}\left(\frac{1}{p_1^+ - k^+} + \frac{1}{2p_1^+} + \frac{k^+}{2p_1^+p_2^+}\right) = (-)\tfrac{1}{2}(-\tfrac{1}{2}C_A + C_f)\frac{g^2}{2\pi^2}\left(-\ln\frac{p_1^+}{p_2^+} - \frac{1}{2} + \frac{p_2^+}{2p_1^+}\right)\ln\frac{\Lambda}{\mu}. \tag{4.10}$$

The contribution from Fig. 4(e) is

$$M_{4(e)} = (-\tfrac{1}{2}C_A + C_f)\ (-)\ \frac{p_1^+ p_2^+}{q^+} \frac{g^2}{2(2\pi)^3} \int \frac{d^2\kappa}{\kappa^2} \int_0^{q^+} dk^+ \frac{1}{(p_1^+ - k^+)^2}$$

$$= (-)(-\tfrac{1}{2}C_A + C_f) \frac{g^2}{2\pi^2} \ln \frac{\Lambda}{\mu}. \tag{4.11}$$

Adding the various contributions we have

$$M_{4(a)} + M_{4(d)} + M_{4(e)} = (-\tfrac{1}{2}C_A + C_f) \frac{g^2}{8\pi^2} \left[2 \ln \frac{p_1^+ p_2^+}{\epsilon^2} - 3 + 2 \right] \ln \frac{\Lambda}{\mu}. \tag{4.12}$$

Next we consider contributions from Fig. 5. The contribution from Fig. 5(a) is

$$M_{5(a)} = (-)\frac{1}{2} C_A \frac{g^2}{2(2\pi)^3} \int \frac{d^2\kappa}{\kappa^2} \int_0^{p_2^+} dk^+ k^+ \left[\frac{2k^+}{p_2^+ q_1^+} \left(\frac{1}{q_2^+} - \frac{2}{q_1^+} \right) - \frac{2k^+}{p_1^+ q_2^+} \left(-\frac{1}{q_1^+} + \frac{2}{q_2^+} \right) \right.$$

$$\left. - \frac{2}{q_1^+} \left(\frac{1}{q_2^+} - \frac{2}{q_1^+} \right) + \frac{2}{q_2^+} \left(-\frac{1}{q_1^+} + \frac{2}{q_2^+} \right) + \frac{1}{p_1^+ p_2^+} \frac{2(q^+)^2}{q_1^+ q_2^+} + \frac{2}{q^+} \left(\frac{q_1^+}{q_2^+ p_1^+} - \frac{q_2^+}{q_1^+ p_2^+} \right) \right],$$

where $q_1 = p_1 - k$ and $q_2 = p_2 - k$,

$$= (-)\frac{1}{2} C_A \frac{g^2}{8\pi^2} \left(\frac{4q^+ p_2^+}{p_1^+ \epsilon} - 2 \ln \frac{p_1^+ p_2^+}{q^+ \epsilon} + \frac{6p_2^+}{p_1^+} \ln \frac{p_2^+}{\epsilon} + \frac{6p_1^+}{p_2^+} \ln \frac{p_1^+}{q^+} - 12 - \frac{p_2^+}{p_1^+} \right) \ln \frac{\Lambda}{\mu}. \tag{4.13}$$

Here we first encounter a *linear* infrared divergence in the one-loop calculation of the vertex in addition to the mixing term. The contribution from Fig. 5(b) is

$$M_{5(b)} = (-)\frac{1}{2} C_A \frac{p_2^+}{q^+} \frac{g^2}{2(2\pi)^3} \int \frac{d^2\kappa}{\kappa^2}$$

$$\times \int_0^{q^+} dk^+ k^+ \left[\frac{-2(p_1^+ - k^+)}{p_2^+ k^+} \left(\frac{1}{(q^+ - k^+)} + \frac{2}{k^+} \right) - \frac{2(p_1^+ - k^+)}{p_1^+ (q^+ - k^+)} \left(\frac{1}{k^+} + \frac{2}{(q^+ - k^+)} \right) \right.$$

$$- \frac{2}{k^+} \left(-\frac{1}{(q^+ - k^+)} - \frac{2}{k^+} \right) - \frac{2}{(q^+ - k^+)} \left(-\frac{1}{k^+} - \frac{2}{(q^+ - k^+)} \right)$$

$$\left. - \frac{1}{p_1^+ p_2^+} \frac{2(q^+)^2}{k^+ (q^+ - k^+)} + \frac{2}{k^+ (q^+ - k^+)} \left(\frac{(p_1^+ - k^+)^2}{p_1^+ p_2^+} - 1 \right) \right]$$

$$= (-)\frac{1}{2} C_A \frac{g^2}{8\pi^2} \left(\frac{4q^+ p_2^+}{p_1^+ \epsilon} - 6 \ln \frac{q^+}{\epsilon} - 6 \frac{p_2^+}{p_1} \ln \frac{q^+}{\epsilon} + 3 + \frac{p_2^+}{p_1^+} \right) \ln \frac{\Lambda}{\mu}. \tag{4.14}$$

Note the presence of linear infrared divergence in this contribution. The contribution from Fig. 5(c) is

$$M_{5(c)} = 0. \tag{4.15}$$

The contribution from Fig. 5(d) is

$$M_{5(d)} = C_A \frac{p_2^+}{p_1^+ q^+} \frac{g^2}{2(2\pi)^3} \int \frac{d^2\kappa}{\kappa^2}$$

$$\times \int_0^{p_1^+} dk^+ k^+ \frac{(q^+ + k^+)}{(q^+ - k^+)^2}.$$

$$= C_A \frac{g^2}{8\pi^2} \left(\frac{4q^+ p_2^+}{p_1^+ \epsilon} - \frac{3p_2^+}{p_1^+} \ln \frac{q^+}{p_2^+} - 2 + \frac{p_2^+}{q^+} \right) \ln \frac{\Lambda}{\mu}. \tag{4.16}$$

It is reassuring to see that the linear infrared divergences cancel between Figs. 5(a), 5(b), and 5(d). The contribution from Fig. 5(e) is

$$M_{5(e)} = C_A \frac{g^2}{2(2\pi)^3} \frac{p_1^+}{q^+ p_2^+} \int \frac{d^2\kappa}{\kappa^2} \int_0^{p_2^+} dk^+ k^+ \frac{(q^+ - k^+)}{(q^+ + k^+)^2}$$

$$= C_A \frac{g^2}{8\pi^2} \left(\frac{3p_1^+}{p_2^+} \ln \frac{p_1^+}{q^+} - 2 - \frac{p_1^+}{q^+} \right) \ln \frac{\Lambda}{\mu}. \tag{4.17}$$

Adding various contributions we have

$$M_{5(a)} + M_{5(b)} + M_{5(d)} + M_{5(e)}$$

$$= (-)\frac{1}{2} C_A \frac{g^2}{8\pi^2} \left(1 - 2 \ln \frac{p_1^+ p_2^+}{\epsilon^2} - 4 \ln \frac{q^+}{\epsilon} \right) \ln \frac{\Lambda}{\mu}. \tag{4.18}$$

The contribution from Fig. 6(a) is

$$M_{6(a)} = (-)\ 2\ \frac{p_2^+}{q^+}\frac{g^2}{2(2\pi)^3}C_f \int \frac{d^2\kappa}{\kappa^2}\int_0^{p_1^+} dk^+ \frac{1}{p_1^+}\frac{k^+}{p_1^+}$$
$$= (-)\ \frac{p_2^+}{q^+}\frac{g^2}{8\pi^2}C_f \ln\frac{\Lambda}{\mu}. \tag{4.19}$$

The contribution from Fig. 6(b) is

$$M_{6(b)} = 2\ \frac{p_1^+}{q^+}\frac{g^2}{2(2\pi)^3}C_f \int \frac{d^2\kappa}{\kappa^2}\int_0^{p_2^+} dk^+ \frac{1}{p_2^+}\frac{k^+}{p_2^+}$$
$$= \frac{p_1^+}{q^+}\frac{g^2}{8\pi^2}C_f \ln\frac{\Lambda}{\mu}. \tag{4.20}$$

The combined contribution from Fig. 6 is

$$M_6 = \frac{g^2}{8\pi^2}C_f \ln\frac{\Lambda}{\mu}. \tag{4.21}$$

The contributions from Fig. 7 are

$$M_{7(a)} = 0, \tag{4.22}$$

$$M_{7(b)} = 0. \tag{4.23}$$

In order to evaluate the contributions to the coupling constant we have to multiply M_2 and M_3 by a factor of $\frac{1}{2}$ [33,34] [also see Eq. (3.33) in paper II]. Thus adding the contributions, we have

$$\delta\mathcal{M}_{02} = \left\{\tfrac{1}{2}M_2 + \tfrac{1}{2}M_3 + M_4 + M_5 + M_6 + M_7\right\}\mathcal{M}_{02}$$
$$= imgT^a_{\beta\alpha}\left(\frac{1}{p_1^+} - \frac{1}{p_2^+}\right)\chi^\dagger_{\lambda_2}\sigma^\perp\cdot\epsilon^\perp_\sigma\chi_{\lambda_1}\left(\frac{11}{3}C_A - \frac{4}{3}N_fT_f\right)\frac{g^2}{16\pi^2}\ln\frac{\Lambda}{\mu}$$
$$+imgT^a_{\beta\alpha}\left(\frac{1}{p_1^+} - \frac{1}{p_2^+}\right)\chi^\dagger_{\lambda_2}\sigma^\perp\cdot\epsilon^\perp_\sigma\chi_{\lambda_1}\left[2C_f + C_f\right]\frac{g^2}{8\pi^2}\ln\frac{\Lambda}{\mu}. \tag{4.24}$$

Recalling our discussion in Sec. II, we identify the first term in the above expression as the coupling constant correction and the second term as the "vertex mass" correction. Comparison with Eq. (3.23) in Sec. III shows that we get the same β function. An additional divergence however appears in the vertex as we anticipated in Sec. II. The "vertex mass" correction is

$$\delta m = \frac{3g^2}{8\pi^2}C_f \ln\frac{\Lambda}{\mu}. \tag{4.25}$$

This is exactly the mass correction expected in covariant theory for the mass counterterm. It is in fact surprising to see this factor emerging as the vertex counterterm in the light-front calculation since it is impossible to reproduce the covariant answer for the mass counterterm using the cutoffs we have employed in this paper (see paper II for details). This aspect of regularization and renormalization seems worthy of further investigation in the future.

V. DISCUSSION, CONCLUSIONS, AND OUTLOOK

In this work we continue our study of light-front QCD in the framework of old-fashioned perturbation theory, which was initiated in paper II. We study radiative corrections to the quark-gluon coupling constant. We are motivated by (a) the investigation of the origin of antiscreening in non-Abelian gauge theory in different gauges, especially the origin of antiscreening in a Hamiltonian formulation with only physical degrees of freedom, (b) the study of high energy inclusive and exclusive reactions in QCD and the associated issues of regularization and renormalization in old-fashioned light-front perturbation theory in light-front gauge $A^+ = 0$, and (c) the identification of distinct intermediate Fock-space state contributions to the origin of antiscreening and its implications for bound-state calculations in non-Abelian gauge theory within a truncated Fock-space.

In paper II we studied quark and gluon mass and wave function renormalizations for different regularization schemes. In this work we have restricted ourselves to the simplest choice in a Hamiltonian calculation, namely, we use a principal value prescription for k^+ and a low and high cutoff for $k^\perp$ ($\mu < k^\perp < \Lambda$).

The most obvious feature of our regularization scheme is the appearance of the product of divergences $[\ln(\epsilon)\ln(\Lambda)]$. As we have discussed in paper II, in a Hamiltonian calculation with only physical degrees of freedom and a trivial vacuum, second-order perturbation theory indicates that the quark and gluon wave function renormalization constants should be less than one. It is the presence of a product of divergences that ensures this in the present calculation. As a result we cannot extract the running coupling constant simply from the gluon self-energy. This appears to be a major complaint against the principal value prescription. It is worthwhile to remember that in axial gauge in a covariant calculation it is the particular regularization of the $\frac{1}{(k_3)^2}$ gauge singularity that enables one to extract the running coupling constant from the gluon self-energy [12]. In the present case, although individual contributions exhibit the product of singularities, as we have shown explicitly, they are canceled in an order g^3 calculation of the renormalization of the quark-gluon coupling constant.

Another feature of our regularization is the momentum dependence of the wave function renormalization "constants." This has been noticed before in various contests [16,17,35]. The unusual momentum dependence seems to be a general feature of light-front gauge and the principal value prescription. In axial gauge the renormalization factors are also not pure numbers (they depend on $q \cdot \eta$), but their ultraviolet divergent parts are independent of $q \cdot \eta$ [12,36].

A source of difficulty in the present calculations is the infrared problem caused by massless gluons. This problem appears severely in diagrams involving the three-gluon coupling. Note that in the present formulation infrared problems appear in both small k^+ and small $k^\perp$. We avoid the small $k^\perp$ infrared problem by choosing the lower cutoff on transverse momentum, μ, to be much larger than all the masses in the problem. Since we are mainly interested in the ultraviolet divergences in the present work, we have ignored pure $\ln(\epsilon)$ divergences. In this context we direct the reader's attention to the detailed discussion of wave function renormalization presented in paper II. We have shown that it is possible to get $\ln(\epsilon)$, $\ln(\Lambda)$, and $\ln(\epsilon)\ln(\Lambda)$ divergences in fermion wave function renormalization, depending on the regularization scheme. It is worthwhile to remember that even in covariant gauge calculations [37] of the vertex correction in QCD with dimensional regularization, pure infrared divergences occur which do not get canceled.

In the present work we have addressed only the ultraviolet renormalization of the masses, wave functions, and quark-gluon vertex in light-front QCD. To order g^2, we have already generated a gluon mass counterterm (see paper II) which is absent in the canonical Hamiltonian. The implications of this for the light-front infrared divergence problem and corresponding renormalization in the next order has to be studied prior to the application of the renormalized Hamiltonian to bound-state problems. Work in this direction is in progress. In the future one would also like to study coupling constant renormalization in other regularization schemes and/or perturbation theory schemes in the Hamiltonian context. Note that our calculation had to utilize two cutoffs in transverse momentum (the lower cutoff itself has to be very much greater than particle masses) in order to reproduce well-known results. This feature follows naturally in a renormalization group approach which is also a very promising framework to perform nonperturbative bound-state calculations in reliable approximation schemes. Some of the recent attempts in this direction are Refs. [38–40]. A further avenue of research is the extraction of mass singularities in the context of scale evolution of structure functions in old-fashioned perturbation theory. The study of composite field renormalization, which is essential for the investigation of high-energy QCD, is also an unexplored territory in old-fashioned perturbation theory.

Lastly we mention the most important problem in light-front QCD, namely, the calculation of hadronic bound states. Previous studies of bound states in gauge theories in the light-front formulation in 3+1 dimensions have truncated the Fock space to two fermions and two fermions plus one boson. After this truncation one ignores self-energy and retardation effects to avoid the infrared singularity problem in the bound-state calculation. Such a scheme is appropriate for the calculation of weakly coupled bound states such as in QED. In QCD we expect strongly coupled bound states and because of asymptotic freedom it is possible to have such states even with weak renormalized coupling. Thus bound-state calculations should incorporate the effect of asymptotic freedom in order to ensure meaningful results. This is a nontrivial problem with the truncation of states which is inevitable in any practical calculation. Our calculation of radiative corrections to the quark-gluon coupling constant in old-fashioned light-front perturbation theory in QCD has clearly exhibited the contributions from distinct intermediate Fock-space sectors. This calculation will undoubtedly aid in the program toward the construction of an effective Hamiltonian for hadronic bound states.

ACKNOWLEDGMENTS

We are grateful to R. J. Perry and K. G. Wilson for many valuable comments and insightful discussions. Using the formalism of Lepage and Brodsky with a few corrections R. J. Perry has independently arrived at the final results, a brief summary of which has already been presented [7]. We would also like to acknowledge helpful discussions with R. J. Furnstahl, D. Mustaki, S. Pinsky, J. Shigemitsu, and T. S. Walhout. We want to especially thank R. J. Perry and T. Walhout for their careful reading of the manuscript. This research was supported by National Science Foundation under Grants Nos. PHY-9102922, PHY-8858250, PHY-9203145, and PHY-9207889. The figures in this paper were constructed using the package "FEYNMAN: A LaTeX Routine for Generating Feynman Diagrams" by Michael Levine, Cavendish-HEP 88/11.

APPENDIX

In this appendix we give the explicit expressions for the diagrams in Figs. 2–7 using the rules developed in paper II for old-fashioned light-front QCD perturbation theory. In writing the above expressions by using the rules, we have used the completeness of the normalized spinors and polarization vectors for the internal quark and gluon lines: $\sum_\lambda \chi_\lambda \chi_\lambda^\dagger = I$ and $\sum_\sigma \epsilon_\sigma^{i*} \epsilon_\sigma^j = \delta_{ij}$. As already noted, P_1^- denotes the off-mass shell light-front energy of the initial quark state. We denote the measure by $d^3[k] = \frac{dk^+ d^2 k^\perp}{2(2\pi)^3}$.

Figures 2(a) and 2(b) contribute to quark wave function renormalization:

$$M_{2(a)} = \int d^3[k]\frac{\theta(k^+)}{k^+}\theta(p_1^+ - k^+)\chi^\dagger(-g)T^a_{\beta\gamma}\Gamma^i_{q0}(p_1, p_2, q)$$
$$\times(-g)T^b_{\gamma\gamma'}\Gamma^j_{q0}(p_1 - k, p_1, -k)(-g)T^b_{\gamma'\alpha}\Gamma^j_{q0}(p_1, p_1 - k, k)\chi\epsilon^{i*}$$
$$\times\frac{1}{[P_1^- - k^- - (p_1 - k)^-](P_1^- - p_1^-)}, \tag{A1}$$

$$M_{2(b)} = \int d^3[k]\frac{\theta(k^+)}{k^+}\theta(p_2^+ - k^+)\chi^\dagger(-g)T^b_{\beta\gamma}\Gamma^j_{q0}(p_2 - k, p_2, -k)$$
$$\times(-g)T^b_{\gamma\gamma'}\Gamma^j_{q0}(p_2, p_2 - k, k)(-g)T^a_{\gamma'\alpha}\Gamma^i_{q0}(p_1, p_2, q)\chi\epsilon^{i*}$$
$$\times\frac{1}{[P_1^- - k^- - (p_1 - k)^-][P_1^- - q^- - k^- - (p_2 - k)^-]}. \tag{A2}$$

Figures 3(a) and 3(b) contribute to gluon wave function renormalization via intermediate fermion-antifermion and two-gluon states, respectively:

$$M_{3(a)} = \int d^3[k]\frac{\theta(q^+)}{q^+}\theta(q^+ - k^+)\theta(k^+)\chi^\dagger(-g)T^a_{\gamma\gamma'}\Gamma^i_{q0}(k, k - q, q)$$
$$\times(-g)T^b_{\gamma'\gamma}\Gamma^j_{q0}(k - q, k, -q)(-g)T^b_{\beta\alpha}\Gamma^j_{q0}(p_1, p_2, q)\chi\epsilon^{i*}$$
$$\times\frac{1}{(P_1^- - k^- - p_2^-)[P_1^- - k^- - (q - k)^- - p_2^-]}, \tag{A3}$$

$$M_{3(b)} = \frac{1}{2}\int d^3[k]\frac{\theta(k^+)}{k^+}\frac{\theta(q^+ - k^+)}{q^+ - k^+}\frac{\theta(q^+)}{q^+}\chi^\dagger(-ig)f^{abc}\Gamma^{ilm}_{g0}(q, -k, k - q)$$
$$\times(-ig)f^{dcb}\Gamma^{jml}_{g0}(-q, q - k, k)(-g)T^d_{\beta\alpha}\Gamma^j_{q0}(p_1, p_2, q)\chi\epsilon^{i*}$$
$$\times\frac{1}{(P_1^- - k^- - p_2^-)[P_1^- - k^- - (q - k)^- - p_2^-]}. \tag{A4}$$

Figures 4(a)–4(e) involve various vertex corrections involving quark-gluon vertex:

$$M_{4(a)} = \int d^3[k]\frac{\theta(k^+)}{p_2^+ - k^+}\theta(p_2^+ - k^+)\chi^\dagger(-g)T^b_{\beta\gamma}\Gamma^j_{q0}(k, p_2, k - p_2)$$
$$\times(-g)T^a_{\gamma\gamma'}\Gamma^i_{q0}(k + q, k, q)(-g)T^b_{\gamma'\alpha}\Gamma^j_{q0}(p_1, k + q, p_2 - k)\chi\epsilon^{i*}$$
$$\times\frac{1}{[P_1^- - (k + q)^- - (p_2 - k)^-][P_1^- - q^- - k^- - (p_2 - k)^-]}, \tag{A5}$$

$$M_{4(b)} = \int d^3[k]\frac{\theta(k^+)}{k^+}\theta(p_2^+ - k^+)\chi^\dagger(-g)T^b_{\beta\gamma}\Gamma^j_{q0}(p_2 - k, p_2, -k)$$
$$\times g^2\frac{(T^aT^b)_{\gamma\alpha}\sigma^i\sigma^j}{p_2^+ + q^+ - k^+}\chi\epsilon^{i*}\frac{1}{P_1^- - q^- - k^- - (p_2 - k)^-}, \tag{A6}$$

$$M_{4(c)} = \int d^3[k]\frac{\theta(k^+)}{k^+}\theta(p_1^+ - k^+)\chi^\dagger g^2\frac{(T^bT^a)_{\beta\gamma}\sigma^j\sigma^i}{p_1^+ - q^+ - k^+}$$
$$\times(-g)T^b_{\gamma\alpha}\Gamma^j_{q0}(p_1, p_1 - k, k)\chi\epsilon^{i*}\frac{1}{P_1^- - k^- - (p_1 - k)^-}, \tag{A7}$$

$$M_{4(d)} = \int d^3[k]\frac{\theta(k^+)}{p_1^+ - k^+}\theta(q^+ - k^+)\chi^\dagger(-g)T^b_{\beta\gamma}\Gamma^j_{q0}(k - q, p_2, k - p_1)$$
$$\times(-g)T^a_{\gamma\gamma'}\Gamma^i_{q0}(k, k - q, q)(-g)T^b_{\gamma'\alpha}\Gamma^j_{q0}(p_1, k, p_1 - k)\chi\epsilon^{i*}$$
$$\times\frac{1}{[P_1^- - k^- - (p_1 - k)^-][P_1^- - p_2^- - (k)^- - (q - k)^-]}, \tag{A8}$$

$$M_{4(e)} = \int d^3[k]\theta(k^+)\theta(q^+ - k^+)\chi^\dagger(-g)T^a_{\gamma\gamma'}\Gamma^i_{q0}(k, k - q, q)$$
$$\times 4g^2T^b_{\beta\gamma}T^b_{\gamma'\alpha}\frac{1}{(p_1^+ - k^+)^2}\chi\epsilon^{i*}\frac{1}{P_1^- - k^- - (q - k)^- - p_2^-}. \tag{A9}$$

Figures 5(a)–5(e) represent vertex corrections involving the three-gluon vertex:

$$M_{5(\mathrm{a})} = \int d^3[k]\theta(k^+)\frac{\theta(p_1^+ - k^+)}{p_1^+ - k^+}\frac{\theta(p_2^+ - k^+)}{p_2^+ - k^+}\chi^\dagger(-g)T^b_{\beta\gamma}\Gamma^l_{q0}(k,p_2,k-p_2)$$
$$\times(-ig)f^{acb}\Gamma^{ijl}_{g0}(q,k-p_1,p_2-k)(-g)T^c_{\gamma\alpha}\Gamma^j_{q0}(p_1,k,p_1-k)\chi\epsilon^{i*}$$
$$\times\frac{1}{[P_1^- - k^- - (p_1-k)^-][P_1^- - q^- - (p_2-k)^- - k^-]}, \tag{A10}$$

$$M_{5(\mathrm{b})} = \int d^3[k]\frac{\theta(k^+)}{k^+}\theta(p_1^+ - k^+)\frac{\theta(q^+ - k^+)}{q^+ - k^+}\chi^\dagger(-ig)f^{acb}\Gamma^{ijl}_{g0}(q,-k,k-q)$$
$$\times(-g)T^b_{\beta\gamma}\Gamma^l_{q0}(p_1-k,p_2,q-k)(-g)T^c_{\gamma\alpha}\Gamma^j_{q0}(p_1,p_1-k,k)\chi\epsilon^{i*}$$
$$\times\frac{1}{[P_1^- - k^- - (p_1-k)^-][P_1^- - k^- - (q-k)^- - p_2^-]}, \tag{A11}$$

$$M_{5(\mathrm{c})} = \int d^3[k]\frac{\theta(k^+)}{[k^+]}\frac{\theta(q^+ - k^+)}{q^+ - k^+}\chi^\dagger(-ig)f^{abc}\Gamma^{ijl}_{g0}(q,-k,k-q)$$
$$\times g^2\frac{(T^cT^b)_{\beta\alpha}\sigma^l\sigma^j}{p_1^+ - k^+}\chi\epsilon^{i*}\frac{1}{P_1^- - k^- - (q-k)^- - p_2^-}, \tag{A12}$$

$$M_{5(\mathrm{d})} = \int d^3[k]\frac{\theta(k^+)}{k^+}\theta(p_1^+ - k^+)\chi^\dagger(-2ig^2)T^b_{\beta\gamma}f^{bca}\frac{-(q^+ + k^+)}{(q^+ - k^+)^2}$$
$$\times(-g)T^c_{\gamma\alpha}\Gamma^i_{q0}(p_1,p_1-k,k)\chi\epsilon^{i*}\frac{1}{P_1^- - k^- - (p_1-k)^-}, \tag{A13}$$

$$M_{5(\mathrm{e})} = \int d^3[k]\frac{\theta(k^+)}{k^+}\theta(p_2^+ - k^+)\chi^\dagger(-g)T^c_{\beta\gamma}\Gamma^i_{q0}(p_2-k,p_2,-k)$$
$$\times(-2ig^2)T^b_{\gamma\alpha}f^{bac}\frac{q^+ - k^+}{(q^+ + k^+)^2}\chi\epsilon^{i*}\frac{1}{P_1^- - q^- - k^- - (p_2-k)^-}. \tag{A14}$$

Figures 6(a) and 6(b) contribute to the "vertex mass" renormalization:

$$M_{6(\mathrm{a})} = \int d^3[k]\frac{\theta(k^+)}{k^+}\theta(p_1^+ - k^+)\chi^\dagger g^2\frac{(T^aT^b)_{\beta\gamma}\sigma^i\sigma^j}{p_1^+}$$
$$\times(-g)T^b_{\gamma\alpha}\Gamma^j_{q0}(p_1,p_1-k,k)\chi\epsilon^{i*}\frac{1}{P_1^- - k^- - (p_1-k)^-}, \tag{A15}$$

$$M_{6(\mathrm{b})} = \int d^3[k]\frac{\theta(k^+)}{k^+}\theta(p_2^+ - k^+)\chi^\dagger(-g)T^b_{\beta\gamma}\Gamma^j_{q0}(p_2-k,p_2,-k)$$
$$\times g^2\frac{(T^bT^a)_{\gamma\alpha}\sigma^j\sigma^i}{p_2^+}\chi\epsilon^{i*}\frac{1}{P_1^- - q^- - k^- - (p_2-k)^-}. \tag{A16}$$

Figures 7(a) and 7(b) represent contributions to the vertex arising from an intermediate instantaneous gluon attached to the initial quark state:

$$M_{7(\mathrm{a})} = \int d^3[k]\theta(q^+ - k^+)\theta(k^+)\chi^\dagger(-g)T^a_{\gamma\gamma'}\Gamma^i_{q0}(k,k-q,q)$$
$$\times(4g^2)T^b_{\gamma'\gamma}T^d_{\beta\alpha}\frac{1}{(q^+)^2}\chi\epsilon^{i*}\frac{1}{P_1^- - k^- - (q-k)^- - p_2^-}, \tag{A17}$$

$$M_{7(\mathrm{b})} = \frac{1}{2}\int d^3[k]\frac{\theta(k^+)}{k^+}\frac{\theta(q^+ - k^+)}{q^+ - k^+}\chi^\dagger(-ig)f^{abc}\Gamma^{ilm}_{g0}(q,-k,k-q)$$
$$\times(-2ig^2)f^{dbc}T^d_{\beta\alpha}\frac{2k^+ - q^+}{(q^+)^2}\chi\epsilon^{i*}\frac{1}{P_1^- - k^- - (q-k)^- - p_2^-}. \tag{A18}$$

[1] Some early references are S. Weinberg, Phys. Rev. **150**, 1313 (1966); G. Feldman, G. Fulton, and J. Townsend, Phys. Rev. D **7**, 1814 (1973); C.B. Thorn, *ibid.* **20**, 1435 (1979).
[2] R.J. Perry, A. Harindranath, and K.G. Wilson, Phys. Rev. Lett. **65**, 2559 (1990). An extensive list of references on light-front physics is available via anonymous ftp from pacific.mps.ohio-state.edu under the subdirectory pub/infolight.
[3] For reviews see X. Ji, Comments Nucl. Part. Phys. **21**, 123 (1993); S.J. Brodsky, G. McCartor, H.C. Pauli, and S. Pinsky, Particle World **3**, 109 (1993).
[4] Wei-Min Zhang and Avaroth Harindranath, this issue, Phys. Rev. D **48**, 4868 (1993).
[5] Wei-Min Zhang and Avaroth Harindranath, Phys. Lett. B **314**, 223 (1993).
[6] Wei-Min Zhang and Avaroth Harindranath, preceding paper, Phys. Rev. D **48**, 4881 (1993).
[7] R.J. Perry, Phys. Lett. B **300**, 8 (1993).
[8] For a very early example of the "wrong sign" of charge renormalization see V.S. Vanyashin and M.V. Terent'ev, Zh. Eksp. Teor. Fiz. **48**, 565 (1965) [Sov. Phys. JETP **21**, 375 (1965)].
[9] D.J. Gross and F. Wilczek, Phys. Rev. Lett. **30**, 1343 (1973).
[10] H. David Politzer, Phys. Rev. Lett. **30**, 1346 (1973).
[11] I.B. Khriplovich, Yad. Fiz. **10**, 409 (1969) [Sov. J. Nucl. Phys. **10**, 235 (1970)].
[12] J. Frenkel and J.C. Taylor, Nucl. Phys. **B109**, 439 (1976).
[13] T. Appelquist, M. Dine, and I.F. Muzinich, Phys. Lett. **69B**, 231 (1977).
[14] T.D. Lee, *Particle Physics and Introduction to Field Theory* (Harwood Academic, New York, 1981).
[15] For a detailed discussion of gluon propagator in axial gauge, see G.B. West, Phys. Rev. D **27**, 1878 (1983).
[16] C.B. Thorn, Phys. Rev. D **20**, 1934 (1979).
[17] G. Curci, W. Furmanski, and R. Petronzio, Nucl. Phys. **B175**, 27 (1980).
[18] S.J. Brodsky, F.E. Close, and J.F. Gunion, Phys. Rev. D **8**, 3679 (1973).
[19] S. Mandelstam, Nucl. Phys. **B213**, 140 (1983).
[20] G. Leibbrandt, Phys. Rev. D **29**, 1699 (1984).
[21] D.M. Capper, J.J. Dulwych, and M.J. Litvak, Nucl. Phys. **B241**, 463 (1984).
[22] H.C. Lee and M.S. Milgram, Nucl. Phys. **B268**, 543 (1986).
[23] A. Bassetto, G. Nardulli, and R. Soldati, *Yang-Mills Theories in Algebraic Non-Covariant Gauges* (World Scientific, Singapore, 1991).
[24] For an attempt toward the implementation of the Mandelstam-Leibbrandt prescription in the light-front bound-state equation, see H.H. Liu and D.E. Soper, Phys. Rev. D **48**, 184 (1993).
[25] K.G. Wilson, "Light front QCD," report (unpublished).
[26] M. Burkardt and A. Langnau, Phys. Rev. D **44**, 3857 (1991); **44**, 1187 (1991); A. Langnau and M. Burkardt, *ibid.* **47**, 3452 (1993).
[27] R.K. Ellis, H. Georgi, M. Machacek, H.D. Politzer, and G.G. Ross, Nucl. Phys. **B152**, 285 (1979).
[28] Yu.L. Dokshitzer, D.I. Dyakonov, and S.I. Troyan, Phys. Rep. **58**, 269 (1980).
[29] S.D. Drell, D.J. Levi, and T.-M. Yan, Phys. Rev. Lett. **22**, 744 (1969); Phys. Rev. **187**, 2159 (1969); Phys. Rev. D **1**, 1035 (1970); **1**, 1617 (1970).
[30] J.D. Bjorken, J.B. Kogut, and D.E. Soper, Phys. Rev. D **3**, 1382 (1971).
[31] S.J. Brodsky and G.P. Lepage, in *Perturbative Quantum Chromodynamics*, edited by A.H. Mueller (World Scientific, Singapore, 1989), p. 93, and references therein.
[32] St. Glazek, A. Harindranath, S. Pinsky, J. Shigemitsu, and K. Wilson, Phys. Rev. D **47**, 1599 (1993).
[33] J.D. Bjorken and S.D. Drell, *Relativistic Quantum Mechanics* (McGraw-Hill, New York, 1964).
[34] W. Heitler, *The Quantum Theory of Radiation* (Oxford University Press, London, 1936).
[35] D. Mustaki, S. Pinsky, J. Shigemitsu, and K. Wilson, Phys. Rev. D **43**, 3411 (1991).
[36] W. Konetschney, Nuovo Cimento **44A**, 465 (1978).
[37] See, for example, R.D. Field, *Applications of Perturbative QCD* (Addison-Wesley, New York, 1989).
[38] B. van de Sande and S. Pinsky, Phys. Rev. D **46**, 5479 (1982).
[39] St. Glazek and K.G. Wilson, Phys. Rev. D **47**, 4657 (1993).
[40] R.J. Perry, "A renormalization group approach to Hamiltonian light-front field theory," OSU Report No. OSU-NT-93-117, 1993 (unpublished).